PART B

Psychophysics, Eye Movements,

Physiological Optics

Vision Res. Vol. 31, No. 4, pp. 649–660, 1991
Printed in Great Britain.

0042-6989/91 $3.00 + 0.00

ON THE HALF-CYCLE DISPLACEMENT LIMIT OF SAMPLED DIRECTIONAL MOTION

WALTER F. BISCHOF and VINCENT DI LOLLO
Department of Psychology, University of Alberta, Edmonton, Alberta, Canada T6G 2E9

(*Received* 5 *March* 1990; *in revised form* 18 *June* 1990)

Abstract—We employed filtered random-dot kinematograms to determine the maximum displacement (d_{max}) at which sampled directional motion was reliably detected. The images were produced using ideal band-pass filters that varied in lower cut-off frequency (f_l), in bandwidth, and in range (α) of component orientations that were passed. Results showed that d_{max}, expressed in cycles of f_l, increased with f_l and α, and decreased with bandwidth. In many conditions, d_{max} exceeded half a cycle of f_l, a result that appears to contradict predictions from quadrature models of motion detection. However, an account that does not violate the half-cycle limit can be given on two assumptions. First, motion perception is mediated by a population of orientation and frequency-selective sensors that respond correctly to displacements up to half a cycle in the preferred direction. Second, the outputs from all sensors (notably including off-axis sensors) are linearly summated to yield perception of motion. A computer simulation based on these assumptions provided a remarkably close fit to the psychophysical data.

Motion perception Motion integration Spatial filtering Kinematograms d_{max}

INTRODUCTION

Apparent motion can be produced by displaying an image in two brief sequential frames (F1 and F2), wherein F2 is a translated version of F1. Under appropriate spatiotemporal conditions, the image is seen to move in the direction of the displacement (e.g. Braddick, 1974). This is known as *discontinuous* or *sampled* motion to distinguish it from *continuous* or *smooth* motion, as seen in the real world.

Perception of sampled motion depends critically on the extent of F1–F2 displacement. Over small displacements, sampled and smooth motion are indistinguishable (Burr, Ross & Morrone, 1986; Watson, Ahumada & Farrell, 1986; Morgan, 1980). At larger displacements, sampled motion continues to be perceived up to a limit—known as d_{max}—beyond which coherent directional motion can no longer be seen reliably.

Several studies have examined the effects of spectral composition of the stimuli on d_{max}. Two outcomes, ostensibly at odds with each other, have been reported for sinusoidal gratings and for bandpass filtered images. With sinusoidal gratings, coherent directional motion is seen up to displacements just short of half a cycle of the grating (Baker, Baydala & Zeitouni, 1989; Bischof & Di Lollo, 1990; Nakayama & Silverman, 1985; Turano & Pantle, 1985). The half-cycle limit defines an inverse scaling between the spatial frequency of the stimulus and d_{max}, expressed in min arc. On this basis, it should be expected that, in an image containing a range of spatial frequencies, the value of d_{max} should be limited by the half-period of the lowest spatial frequency present in the image. For example, consider a compound grating containing three spatial frequency components: 2, 3 and 4 c/deg, with corresponding half-periods of 15, 10 and 7.5 min arc. For the sake of the example, suppose that the system's response were determined solely by the lowest frequency in the image. Given a displacement limit of just under half a cycle, this would yield the highest possible value of d_{max}, namely just under 15 min arc. Even if the higher frequencies were to play a part, no higher value of d_{max} should occur for this image because, to the extent that the system's response is influenced by the higher frequency components, the limiting value of d_{max} would be diminished correspondingly. Such reduction of d_{max} in the presence of higher frequency components has been reported by Cleary and Braddick (1990b).

Expectations regarding the half-cycle limit of d_{max} were not confirmed in recent studies by Bischof and Di Lollo (1990) and by Cleary and Braddick (1990a). Both studies employed pairs of random-dot patterns (known as random-dot

kinematograms) band-pass filtered at different centre frequencies. It was found that d_{max} was considerably greater than the half-period of the lowest frequency in the image, particularly for images of relatively high centre frequencies. On the face of it, the observers were responding to spatial frequencies that were below the limit of the band-pass filter, and hence not present in the image. It must be noted, however, that the filters employed in these studies were isotropic, hence the images contained frequency components of all orientations besides the orientation orthogonal to the direction of motion.

With this in mind, an account of the larger-than-expected values of d_{max} can be given by assuming a population of frequency-tuned orientation-selective motion sensors with an upper displacement limit of half a cycle in the preferred direction (Adelson & Movshon, 1982; Bischof & Di Lollo, 1990; Cleary & Braddick, 1990a). Perception of motion in an arbitrary direction is held to be determined by the combined outputs of all sensors. This model can account for the excessive values of d_{max} in the following way. Illustrated in Fig. 1 is the two-dimensional Fourier domain of an image. Within the frequency band of the ideal band-pass filter represented by the shaded area, S denotes a diagonal frequency component with corresponding vertical frequency v_s and horizontal frequency u_s. As can be seen, u_s is lower than the filter's lower cut-off frequency (f_l), hence its period is greater. Suppose that the system's response to horizontal motion were determined solely by S. In this case, the value of d_{max} would

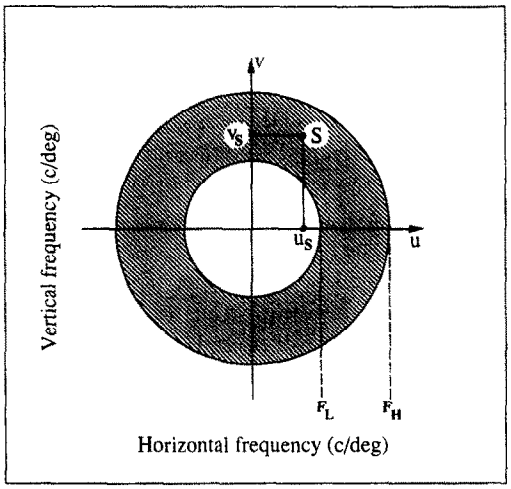

Fig. 1. Two-dimensional Fourier domain of an image, showing an ideal band-pass filter with cut-off frequencies f_l and f_h. Also shown is a diagonal frequency component S with vertical frequency v_s and horizontal frequency u_s.

be just short of half a cycle of u_s and, therefore, greater than the notional limit set by half a cycle of f_l. Just as in the earlier example with the compound grating, the presence of horizontal frequencies higher than u_s might reduce—but never increase—the value of d_{max}.

In a nutshell, this approach accounts for the unexpectedly large values of d_{max} in terms of the horizontal frequencies of the diagonal components in bandpass-filtered images. Two clear predictions follow from this account: first, were all but the horizontal frequency components to be removed from the image, the value of d_{max} should never exceed the half-period of f_l. Second, were the filter to be systematically changed so as to maintain the same bandwidth but to pass increasing amounts of diagonal components, the value of d_{max} should reveal corresponding increments, possibly beyond the nominal limit set by f_l. These, as well as related predictions, are tested in the present work.

EXPERIMENT 1

Methods

Observers. One of the authors and one paid undergraduate student, naive as to the purpose of the study, served as observers. They had normal or corrected-to-normal vision.

Stimuli. The stimuli were bandpass filtered images with a resolution of 128 × 128 pixels. At the viewing distance of 57 cm the square images subtended an angle of 4 deg. Each image contained up to 256 grey levels, and was normalized to a mean luminance of 54 cd/m^2 (including screen luminance of 10 cd/m^2, as explained below) and peak Michelson contrast of 0.56, yielding a range of 24–84 cd/m^2. Each image was constructed from a 128^2 random-dot matrix in which each dot could be either black or white with a probability of 0.5. The images were filtered with one of the three orientation-limited ideal bandpass filters illustrated in Fig. 2. The filter in Fig. 2a passed only components with an orientation of 90 deg, which produced vertical compound gratings. The filter in Fig. 2b had the same centre orientation (90 deg) but had an orientation bandwidth (α) of 90 deg, passing components with orientations between 45 and 135 deg. The third filter (Fig. 2c) was isotropic and therefore passed components of all orientations. Even though, strictly speaking, the centre orientation of the isotropic filter was arbitrary, it is convenient to refer to the three filters as having the same centre orientation of 90 deg and

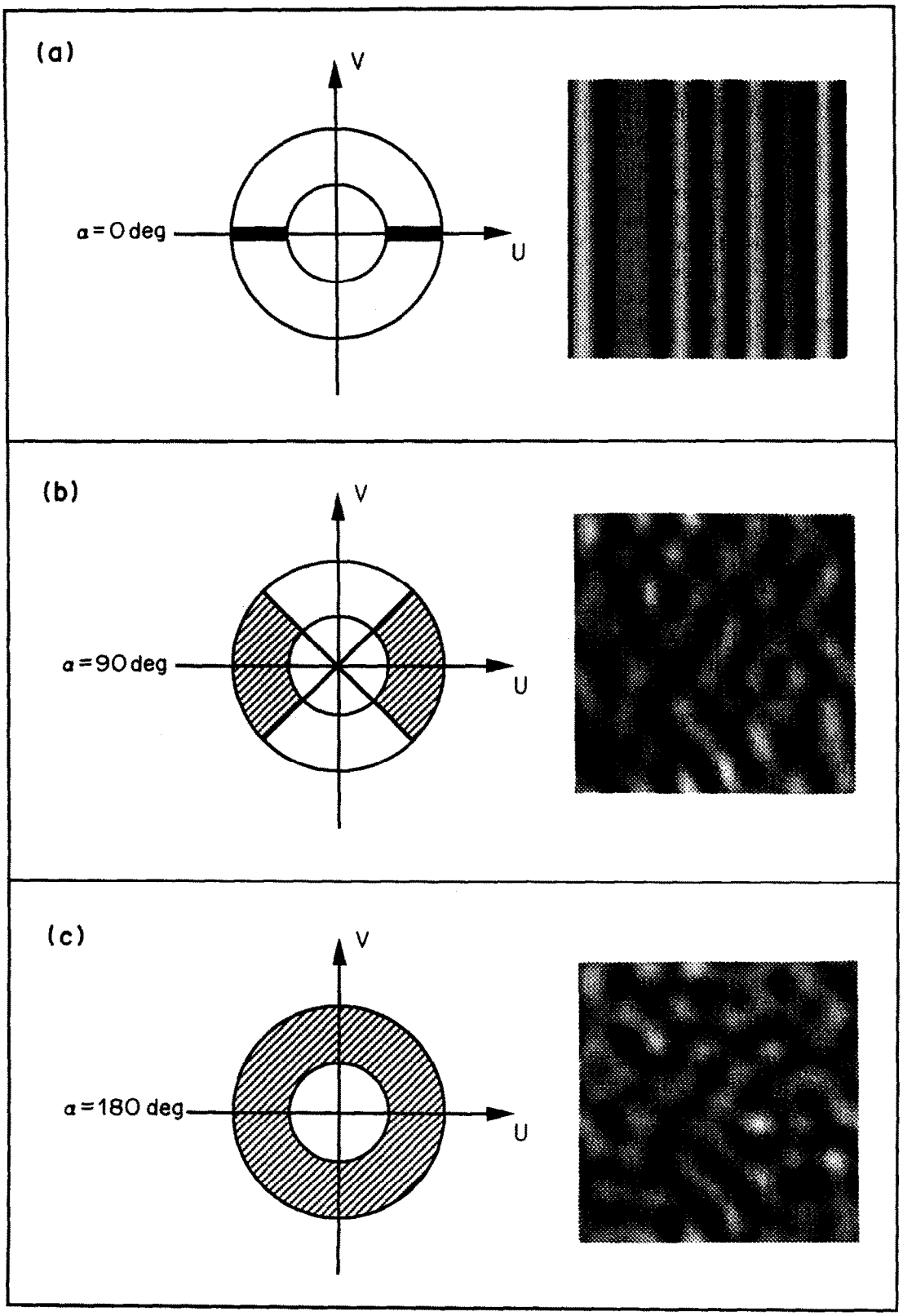

Fig. 2. In the left portion of each panel are the Fourier domains of the filters used to produce the stimuli. All filters had the same centre orientation (90 deg) but different orientation bandwidths (α), as shown. In the right portion of each panel are sample images passed by the corresponding filter with lower cut-off frequency $f_l = 1$ c/deg, and bandwidth 1 octave.

orientation bandwidths of 0, 90 and 180 deg, respectively. Also illustrated in Fig. 2 are sample images filtered by the corresponding orientation-limited filter with bandwidth 1 octave and lower cut-off frequency 1 c/deg. For ease of exposition, the following conventions were adopted in this article: the orientation bandwidth of a filter is denoted as "α". Used without qualifier, the term "bandwidth" refers exclusively to frequency.

Each of the three orientation-limited filters varied in respect to two attributes: bandwidth and lower cut-off frequency (f_l). There were five bandwidths: 0.58, 1, 2, 3 and 4 octaves, and up to seven levels of f_l: 0.5, 0.75, 1, 1.5, 2, 3 and 4 c/deg. In the experimental design, bandwidth was completely crossed with f_l, subject to the restriction that the highest frequency in an image did not exceed 8 c/deg. To avoid effects peculiar to the random structure of any individual image, 20 different images were constructed for each experimental condition defined by bandwidth, orientation bandwidth (α), and f_l. On any one trial, the image to be displayed was chosen randomly from the pool of 20 images.

Apparatus. All stimuli were displayed on a Hewlett–Packard 1332A oscilloscope equipped with fast P15 phosphor. The screen was front-illuminated by a 500-W Sylvania CBA tungsten–halogen projector lamp. A variable neutral-density filter, mounted in the path of the light source, was adjusted to yield an average screen luminance of 10 cd/m^2, as measured by a Spectra Spotmeter. The X, Y and Z (intensity) coordinates of the filtered images were displayed from a fast plotting buffer (Finley, 1985) at the rate of one dot per microsecond. To improve brightness and contrast, each image was plotted four times in succession for a total exposure duration of just under 66 msec.

Procedures. On any given trial, the sequence of events was as follows: the observer sat in a dimly-illuminated chamber and fixated on a cross shown in the centre of the screen. Upon a button-press by the observer, the fixation cross disappeared and the first image (F1) was displayed for 66 msec. Immediately upon termination of F1, the second image (F2) was displayed for 66 msec. The two images were identical except that F2 was displaced horizontally with respect to F1 so as to produce the appearance of motion to the left or to the right, randomly. The parts of F2 that were displaced out of the viewing area by the horizontal shift were "wrapped around" to reappear at the opposite side of the image. The observer indicated the direction of motion by pressing one of two hand-held buttons.

In the present experiments, d_{max} was defined as the F1–F2 displacement that produced 80% correct responses. To obtain values of d_{max} (directly or by interpolation), the range of F1–F2 displacements was adjusted for each observer and condition so as to bracket a level of 80% correct responses. Any given experimental session contained images of only one combination of bandwidth, orientation bandwidth (α), and f_l over the entire range of displacements, in random sequence. In total, each observer made 50 observations for every level of F1–F2 displacement in each experimental condition.

At the end of the experiment, vertical sinusoidal gratings were used to assess each observer's contrast sensitivity function (CSF) under display conditions matching those of the main experiment. Upon a button-press by the observer, two vertical gratings were displayed sequentially for 66 msec each. The two gratings were identical, except that the second was displaced by 0.25 cycles to the left or to the right, randomly. The observer pressed one of two buttons to indicate the direction of motion. Contrast of the gratings was adjusted by a dynamic tracking procedure (PEST, Taylor & Creelman, 1967) to a level that yielded approx. 80% correct responses, which was taken as the threshold of directional motion detection for that spatial frequency. Thresholds estimates were taken at spatial frequencies ranging from 0.5 to 10 c/deg. Figure 3 shows the CSFs for the two observers.

Results

Values of d_{max} for all conditions are shown in Fig. 4. In every case, d_{max} is expressed in cycles of the filter's lower cut-off frequency (f_l) rather than in min arc. This was done for two reasons. First, this representation is intuitively simpler because a null effect of f_l is represented by a curve of zero slope in Fig. 4. Second, it permits

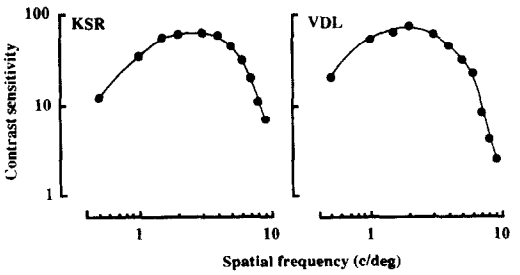

Fig. 3. Contrast sensitivity functions for the two observers.

direct verification of the predictions—outlined in the introduction—regarding the conditions in which d_{max} may exceed hald a cycle of f_l.

For the purpose of the present work, three aspects of the results must be noted.

(1) Increments in orientation bandwidth (α) produced corresponding increments in the values of d_{max}. This can be seen in the relative levels of the three curves within each panel of Fig. 4.

(2) Increments in bandwidth produced corresponding decrements in the values of d_{max}. This can be seen by comparing the levels of corresponding curves across all panels in Fig. 4.

(3) Increments in f_l produced corresponding increments in the values of d_{max}. This can be seen in the slopes of the individual curves in Fig. 4. It must be stressed that d_{max} increases as a function of f_l only when expressed in cycles of f_l, as in Fig. 4. As might be expected, d_{max} would decrease markedly if expressed in min arc. The present results, therefore, are in agreement with the inverse scaling of d_{max} with spatial frequency reported in earlier studies (Bischof & Di Lollo, 1990; Chang & Julesz, 1985; Cleary & Braddick, 1990a). Indeed, where direct comparisons can be made, there is remarkable correspondence between Cleary and Braddick's (1990a) results and ours. We retrieved approximate values of d_{max} from Cleary and Braddick's (1990a) article, and expressed them in cycles of f_l. Cleary and Braddick's values increased as a function of f_l, just as seen in Fig. 4, but were up to 0.2 cycles of f_l higher than in our corresponding conditions. The difference in level can probably be attributed to differences in the luminance of the displays: ours was 54 cd/m^2; that reported by Cleary and Braddick was 35 cd/m^2. As was shown by Dawson and Di Lollo (1990), d_{max} increases sharply as luminance is decreased.

Interpretation of these results in terms of the frequency content of the images is straightforward in some cases, but more complex in others. As an aid to interpretation, and as a means for specifying the underlying assumptions, we developed a simple computer simulation capable of providing a comprehensive account of the results.

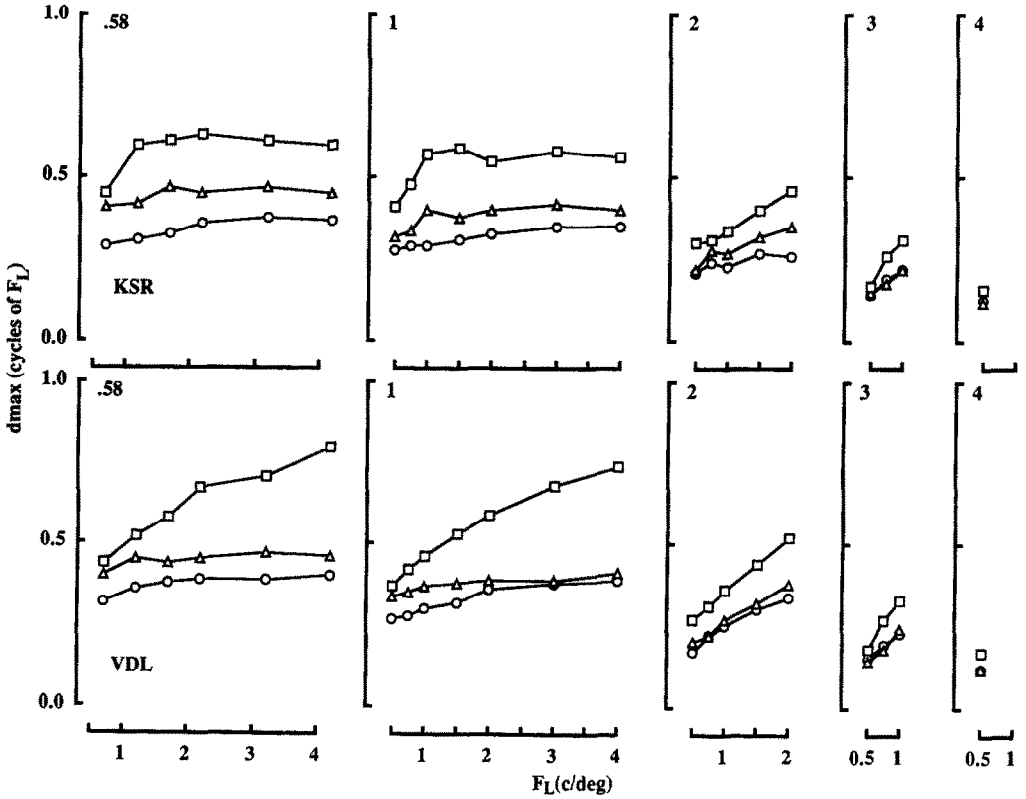

Fig. 4. Values of d_{max} in all experimental conditions for observers KSR (upper panels) and VDL (lower panels). Each value is based on 50 observations, and represents the extent of displacement between leading and trailing frames that produced 80% correct responding. The number at the upper left of each panel indicates filter bandwidth (octaves). Orientation bandwidth of the filter: $\alpha = 0$ deg (○); $\alpha = 90$ deg (△); $\alpha = 180$ deg (□).

Account of the results

Central to the present account is the tenet that d_{max} is proportional to—and can be predicted from—the average horizontal frequency of *all* frequency components of the image. This is in agreement with the reasoning that, in accordance with Fig. 1, the value of d_{max} (expressed in cycles of f_l) increases as components with lower horizontal frequencies are added to the image. On this reasoning, d_{max} should also vary inversely with the average horizontal frequency (μ_u in Fig. 6) of all components of the image. We also hold that all frequency components contribute to perceived motion in weighted measure, according to the observer's CSF.

We implemented these tenets by finding the average horizontal frequency for a given image, having first weighted all frequency components of that image in terms of the observer's CSF.

Let $c(r)$ denote the CSF, where r denotes spatial frequency (see Fig. 3). For simplicity, we assume that the CSF is isotropic. Furthermore, let $F(u, v)$, $0 \leq u, v < n$ denote the discrete Fourier transform of the filters shown in Fig. 2. Then the average horizontal frequency μ_u is defined as:

$$\mu_u = \frac{1}{Z} \sum_{u=1}^{n/2} \sum_{v=0}^{n/2} uw(u, v)F(u, v); \qquad (1)$$

where

$$Z = \sum_{u=1}^{n/2} \sum_{v=0}^{n/2} w(u, v)F(u, v); \qquad (2)$$

and

$$w(u, v) = [\log_2(r + 1) - \log_2(r)]c^2(r)$$
$$r^2 = u^2 + v^2. \qquad (3)$$

Two aspects of the definition of μ_u must be noted. First, the weighting term $w(u, v)$ is used to equalize the frequency components on a logarithmic scale, and to compensate for the effective energy of each frequency component as defined by the CSF. Second, although the power spectra of different images vary randomly, their expected values are, up to a multiplicative constant, equivalent to those of the filters used.

In the implementation, d_{max} was defined as 0.45 cycles of the average horizontal frequency of the image. This was done on the strength of Bischof and Di Lollo's (1990) finding that d_{max} for sinusoidal gratings remains at about 0.45 cycles over a very large range of spatial frequencies. The results of the simulation, using the CSF of observer KSR, are presented in Fig. 5. Virtually identical results were obtained using the CSF of observer VDL.

Comparison of Figs 4 and 5 reveals excellent agreement between obtained and simulated patterns of results. The agreement is all the more remarkable in that the simulation contained no free parameters. The correspondence between the levels of predicted and obtained results was least successful for bandwidths of 0.58 and 1 octave (Figs 4 and 5). It must be noted, however, that these were precisely the conditions that exhibited the most pronounced individual differences in the empirical results. We have obtained improved fits to the individual results by implementing the simulation with anisotropic CSFs, suited to the individual observers. By the same token, while omission of the CSF weightings has only a minor effect on predictions for bandwidths of 0.58 and 1 octaves, it has a major effect at the larger bandwidths. That is, without CSF weighting, the observed effect of f_l (Fig. 4) is not predicted, and the curves for

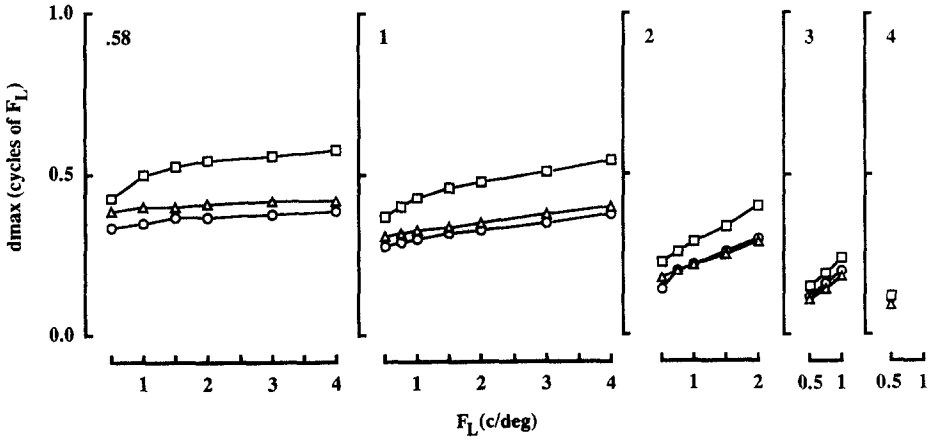

Fig. 5. Results of the computer simulation of the data illustrated in Fig. 4. Symbols are as in Fig. 4.

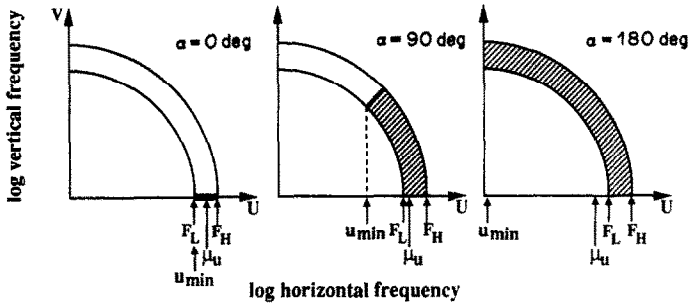

Fig. 6. Upper-right quadrants of the Fourier domains of the three orientation-limited filters used for producing the stimuli. Only one of five possible bandwidths (0.58 octaves) and one of seven possible lower cut-off frequencies of the filter (2 c/deg) are illustrated. The hatched areas indicate the band-pass portions of the filters. Orientation bandwidth of the filter = α; lower frequency cut-off of the filter = f_l; upper cut-off frequency of the filter = f_h; lowest horizontal frequency of any frequency component = u_{min}; average horizontal frequency of all frequency components = μ_u.

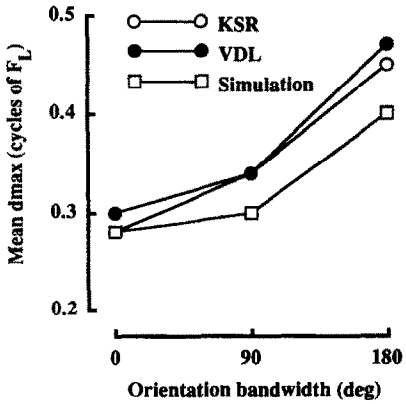

Fig. 7. Mean values of d_{max} in relation to orientation bandwidth of the filter. The circles represent individual results averaged over all 22 conditions within each orientation bandwidth. The squares illustrate the outcome of the computer simulation described in the text.

bandwidths of 2 and 3 octaves in Fig. 5 are uniformly flat.

While permitting an overall comparison between obtained and predicted outcomes, Figs 4 and 5 do not provide a clear and straightforward representation of the effects of the two major variables in the experiment: orientation bandwidth (α) of the filter and filter bandwidth. In addition, the two figures do not provide an intuitively simple representation of the way in which the frequency contents of the images might effect the values of d_{max}. Below, the effects of orientation bandwidth (α) of the filter and filter bandwidth are examined in detail.

Effect of orientation bandwidth. Changes in orientation bandwidth (α) are assumed to affect d_{max} by altering the average horizontal frequency (μ_u) of all components of the image. The relationship between μ_u and α is illustrated in Fig. 6, which contains one quadrant of the Fourier domain of each of the three orientation-limited filters used in the present experiment, with bandwidth and f_l held constant.

It is clear from Fig. 6 that the value of μ_u decreases as α is increased. On this basis, it should be expected that d_{max} should increase correspondingly. This expectation is unambiguously confirmed by the data in Fig. 7, where each point represents the mean of all 22 values of d_{max} obtained at each value of α. For both observers, the mean value of d_{max} increased as orientation bandwidth of the filter was increased. Also shown in Fig. 7 is the outcome of the computer simulation. The good agreement between simulated and empirical data further supports the inference that the limits of motion perception were determined by the average horizontal frequency of all frequency components.

Implied in this conclusion is the proposition that, at displacements that exceeded the half-cycle limit of horizontally-tuned sensors, detection of motion was mediated by sensors tuned to oblique orientations. A similar proposition was explicitly rejected by Cleary and Braddick (1987, 1990a) on the grounds that similar levels of performance are *obtainable* with one-dimensional ($\alpha = 0$ deg) and with two-dimensional ($\alpha = 180$ deg) filtered images. However, the fact that similar levels of performance are *obtainable* under some conditions does not rule out mediation by off-axis sensors. As can be seen in Fig. 4, oblique-orientation components have a strong effect if bandwidth is narrow but not if it is wide (e.g. note the similarity of performance levels when bandwidth is 3 octaves, Fig. 4, fourth panels from the left). Similarity of performance at wide bandwidths is nicely predicted by our simulation based on the mediation of off-axis sensors, as shown in the corresponding panel (fourth from the left) in Fig. 5. According

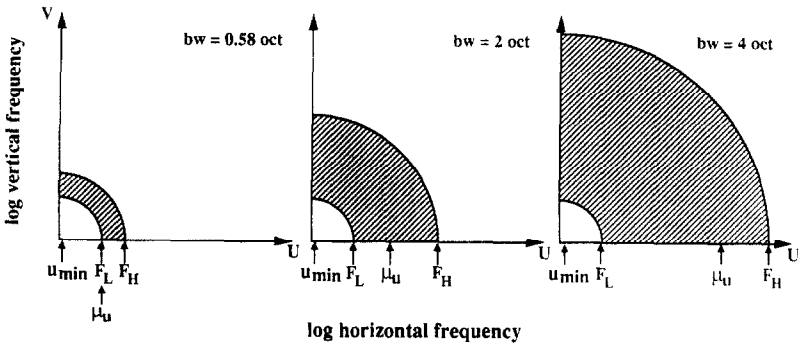

Fig. 8. Upper-right quadrants of the Fourier domains of the filters used for producing the stimuli. Isotropic filters only are illustrated. The lower cut-off frequency (f_l) of the filter in each panel is constant at 0.5 c/deg. Bandwidth (bw) varies across panels, as shown. Upper cut-off frequency of the filter = f_h; lowest horizontal frequency of any frequency component = u_{min}; average horizontal frequency of all frequency components = μ_u.

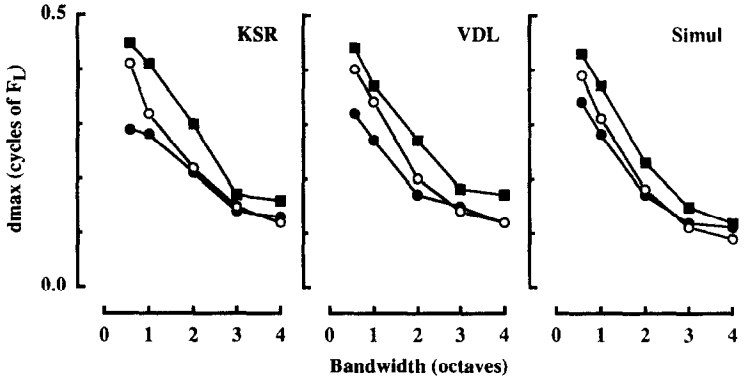

Fig. 9. Values of d_{max} as a function of bandwidth for each orientation bandwidth: $\alpha = 0$ deg (●); $\alpha = 90$ deg (○); $\alpha = 180$ deg (■). Only those values of d_{max} obtained with $f_l = 0.5$ c/deg are illustrated (f_l = lower cut-off frequency of the filter). The panel on the right illustrates the results of the computer simulation described in the text.

to the present analysis, Cleary and Braddick's (1987, 1990a) evidence was likely based on broad-band images, a supposition consistent with Cleary and Braddick's (1987) remark that equality of performance required "sufficient" bandwidth.

Effect of filter bandwidth. For all images with fixed f_l, increments in bandwidth should produce decrements in d_{max}. This follows from two related considerations. The first parallels the argument made in the preceding section. Figure 8, constructed along the lines of Fig. 6, shows that, for a fixed f_l, increments in bandwidth produce corresponding increments in μ_u, hence d_{max} should decrease. The second—purely empirical—consideration is based on Cleary and Braddick's (1990b) finding that perception of motion in the low spatial frequencies is progressively impaired —and the value of d_{max} is progressively diminished—as higher spatial frequencies are added to the image.

In the present experiment, the full effect of bandwidth is best illustrated at the lowest level of f_l. This is so because, in the experimental design, the possible combinations of bandwidth and f_l were subject to the restriction that the highest spatial frequency in the image should not exceed 8 c/deg. Because of this restriction, all five bandwidths could be tested only at the lowest f_l, namely 0.58 c/deg.

An inverse relationship between d_{max} and bandwidth is confirmed in the first two panels of Fig. 9, where all points are the same as in Fig. 4 ($f_l = 0.58$ c/deg), rearranged so as to illustrate the effect of bandwidth, separately for each orientation bandwidth. The right-hand panel of Fig. 9 shows the results of the computer simulation. Separate curves, instead of a single averaged curve for each orientation bandwidth of the filter, are shown in Fig. 9 to underscore the success of the stimulation with detailed aspects of the results, as well as with overall trends.

EXPERIMENT 2

Uniform support was obtained in expt 1 for the proposition that d_{max} is determined by the average *horizontal* frequency (μ_u) of all frequency components of the image. The value of d_{max} was found to increase as more components with lower horizontal frequencies were added to the image. Although plausible, the inferred dependence of d_{max} on μ_u might be questioned because of a possible confounding between μ_u and orientation bandwidth (α). Namely, progressively lower horizontal frequencies were obtained in expt 1 by using filters of correspondingly broader orientation bandwidths.

Unambiguous identification of μ_u as a determinant of d_{max} is, therefore, hindered by the fact that it varied concomitantly with orientation bandwidth (α) in expt 1. Conceivably, the results could have been due to effects related to variations in orientation bandwidth but unrelated to changes in μ_u. Whatever the underlying hypothesis, α and μ_u must be unconfounded if the latter is to be regarded unambiguously as a determinant of d_{max}.

Separation of the two factors was achieved in expt 2 by holding orientation bandwidth constant while varying μ_u. Specifically, we employed a filter with the same orientation bandwidth as the 90 deg filter in expt 1, but with a centre orientation of 0 deg instead of 90 deg. The resulting images, therefore, were simply rotated versions of the corresponding images in expt 1. The plan was to compare the results of expt 2 with the results obtained with the corresponding filter in expt 1. Predictions based on the frequency contents of the images can be made with reference to Fig. 10 which illustrates the Fourier domain of the filter used in expt 2 (panel a), a sample image passed by that filter (panel b), and salient parameters of the filter (panel c). Comparison of Fig. 10 with the corresponding panels in Figs 2 and 6 shows that the two filters are identical in every respect, notably orientation bandwidth, except for μ_u, which has a lower value in Fig. 10. On the assumption that d_{max} is inversely scaled with μ_u, higher values of d_{max} should be found in expt 2 than in the corresponding conditions in expt 1. Indeed, the value of μ_u in Fig. 10 is even lower than that for an orientation bandwidth of 180 deg (Fig. 6, right panel). Therefore, the values of d_{max} obtained in expt 2 should be even higher than the values obtained with an orientation bandwidth of 180 deg in expt 1.

Methods

Observers, apparatus and procedures were the same as in expt 1, with the exception that only one filter was used to produce the images, as shown in Fig. 10. Levels of f_l and bandwidth were the same as in expt 1, as were the procedures for estimating d_{max}.

Results

Values of d_{max} for both observers are illustrated in Fig. 11. To facilitate comparisons, Fig. 11 contains the values of d_{max} for the corresponding condition in expt 1 (i.e. $\alpha = 90$ deg). Also shown in Fig. 11 are the results of the computer simulation.

It is immediately obvious that the levels of d_{max} obtained in expt 2 were higher than the levels obtained in expt 1 not only with $\alpha = 90$ deg, but also (by reference to Fig. 4) with $\alpha = 180$ deg. Both these effects are consistent with the hypothesized inverse scaling between μ_u and d_{max}. Had the principal determinant of d_{max} been orientation bandwidth rather than μ_u, the four empirical curves in Fig. 11 should

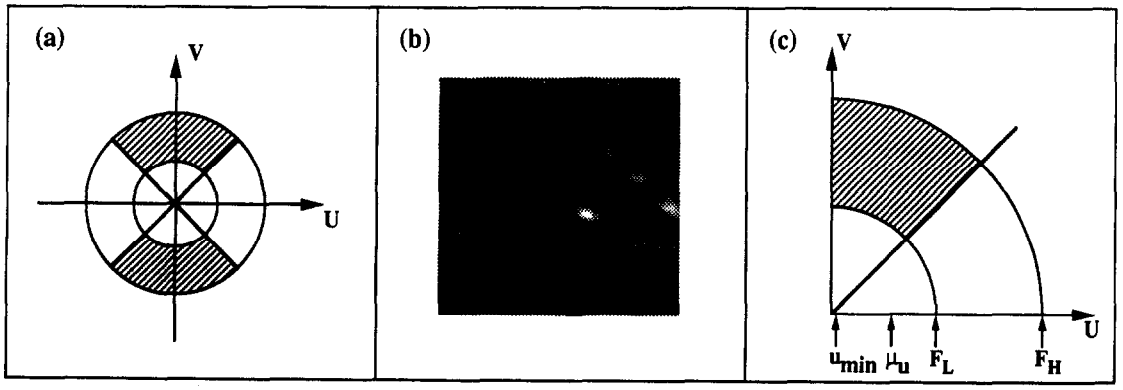

Fig. 10. (a) Fourier domain of a filter used for producing the stimuli in expt 2. (b) Sample image used in expt 2. (c) Upper-right quadrant of the filter illustrated in (a). All symbols are the same as in Fig. 6.

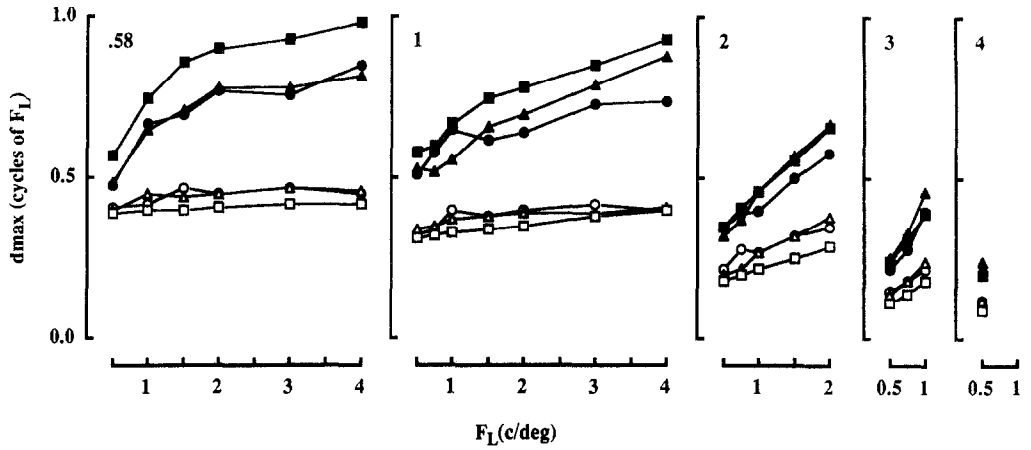

Fig. 11. Values of d_{max} for expt 2 (solid symbols) and for the corresponding conditions ($\alpha = 90$ deg) in expt 1 (open symbols) for observers KSR (circles) and VDL (triangles). The numbers at the upper left of each panel indicates filter bandwidth (octaves). The square symbols represent the results of the computer simulation described in the text.

have been the same. Homologous results have been reported by Chang and Julesz (1983) who attributed the effect to a possible reduction in false matches between F1 and F2 when the elongated blobs in the filtered images lie parallel to the direction of motion.

Also seen in Fig. 11 is a clear interaction effect between filter's centre orientation and f_l. That is, the results of expt 2 show substantially greater increments as a function of f_l than do the results obtained with the corresponding filter in expt 1. Except for some level differences, the interaction was successfully predicted in the simulated results. The remarkable similarity between the obtained and predicted patterns of results confirms the role of μ_u as a determinant of d_{max}, and places strict constraints on alternative explanations.

A comment should be added regarding the interaction effect. Although remarkably close to the obtained results in terms of overall pattern, the simulated values of d_{max} were higher than the obtained values, particularly at the smaller bandwidths (Fig. 11). We are unable to offer a conclusive account of this result. However, it is worth noting that, in the computer simulation, all frequency components in the image were treated as equivalent sources of motion information. This represents optimal efficiency in utilizing the information contained in the image. The lower level of the obtained results strongly suggest that the efficiency of the human observers in utilizing the various frequency components as motion signals is less than optimal. The reasons for this loss in efficiency are beyond the scope of the present experiments.

GENERAL DISCUSSION

Overview of the conceptual framework

Throughout this article, the rationale for the experimental work was based on the conjecture that perception of directional motion can be understood in terms of the frequency contents of the images. Specifically, we examined the proposition that the maximum displacement at which sampled horizontal motion can be seen is determined by the horizontal frequencies of all the frequency components in bandpass-filtered images. We found that detection of sampled motion is related to the spectral contents of the images in a remarkably simple way: motion is seen up to a limit set by the average horizontal frequency (μ_u) of all image components.

The assumptions underlying this combinatorial scheme are equally simple. First, in agreement with Adelson and Movshon (1982), we assume that motion perception is mediated by a population of sensors that are orientation-selective and frequency-tuned. Second, we assume that perception of motion emerges from a linear summation of the outputs from all motion sensors. That is, all sensors are assumed to contribute equally, without nonlinearities such as inhibitory interactions among units adjacent in the frequency domain.

Although a population of motion sensors is assumed in the present scheme, no assumptions are made as to the precise mechanisms of motion detection. In this sense, our scheme is entirely compatible with the major theories of motion detection, be they correlational models (e.g. Reichardt, 1961), energy models (e.g.

Adelson & Bergen, 1985; Van Santen & Sperling, 1985; Watson & Ahumada, 1985), or gradient models (e.g. Marr & Ullman, 1981). Indeed, the present approach could be easily recast within the framework of any of these models.

The half-cycle limit

A tenet common to all models is that the maximum displacement for seeing sampled directional motion (d_{max}) is limited by half a cycle of the spatial frequency to which a given motion sensor is tuned. The half-cycle limit applied also in the present scheme. It was argued in the Introduction that, in a compound vertical grating comprising two or more frequencies, d_{max} is limited by the half-period of the grating with the lowest frequency. More generally, we have argued that d_{max} is limited by the half-period of the lowest horizontal frequency present in an image. In respect to two-dimensional filtered images, we have drawn a crucial distinction between f_l (the lower cut-off frequency of the filter) and u_{min} (the lowest horizontal frequency of any image component). We hold that it is the latter that sets the limit for d_{max}. It should be stressed that there is no corresponding theoretical justification for using f_l as a delimiter of d_{max}. In the present work (e.g. Figs 4 and 11), f_l is used merely for descriptive convenience. In this sense, our use of f_l is equivalent to Cleary and Braddick's (1990a) use of f_c, which refers to the centre frequency of the filter used for producing the images.

So defined, the half-cycle limit was never exceeded in any condition in the present experiments. This can be verified by expressing the data in Fig. 4 in cycles of u_{min} instead of cycles of f_l. No such conversion is required for the condition in which $\alpha = 0$ because, in that case, $f_l = u_{min}$ (see Fig. 6), and the values of d_{max} remain the same when expressed in cycles of u_{min}. In that condition, the highest values of d_{max} were 0.38 and 0.40 cycles of u_{min} for observers KSR and VDL, respectively. In the remaining conditions, the highest values of d_{max} (in cycles of u_{min}) for observers KSR and VDL were: 0.33, 0.33 ($\alpha = 90$ deg, centre orientation = 0 deg); 0.15, 0.15 ($\alpha = 90$ deg, centre orientation = 90 deg); and 0.14, 0.13 ($\alpha = 180$ deg). All these values are substantially lower than the half-cycle limit of 0.5. It may be added that the computer simulation was predicated on the half-cycle (actually, 0.45 cycles) limit for d_{max}. That the limit was not exceeded in the present experiments is further attested by the close correspondence between obtained and simulated results. It goes without saying that the correspondence between simulated and obtained results is invariant with the way in which d_{max} is expressed, be that min arc, cycles of f_l, or cycles of f_c.

Effects of bandwidth: masking or summation?

Given an image passed by a filter with fixed f_l, the value of d_{max} decreases as filter bandwidth is increased (Fig. 9). This result is not new: Cleary and Braddick (1990b) have reported a similar decrement in d_{max} as higher spatial frequencies are added to the image. This outcome was interpreted by Cleary and Braddick as representing a process of masking whereby motion information at the low end of the image's frequency spectrum is masked by the higher frequencies.

Although a mechanism of masking is sufficient for explaining the present results, it is clearly not necessary. In the linear summation scheme proposed here, the decrements in d_{max} are explained simply in terms of corresponding increments in μ_u, as higher spatial frequencies are added to the image. No additional explanatory principles, such as masking or suppression, need be postulated.

This is not to say that we hold the present account to be universally valid, or to discount the option that, under different display conditions, nonlinear mechanisms may play a role in motion perception. However, the results obtained under the conditions employed in the present work—and in related experiments (e.g. Cleary & Braddick, 1990a,b)—are adequately explained by linear summation alone.

Concluding comments

At a most general level, the present work shows that a comprehensive account of motion perception must involve a two-dimensional analysis. Phenomena that are inexplicable in terms of one-dimensional analysis (e.g. the excessive values of d_{max} discussed in the Introduction) are naturally explained in a two-dimensional context.

Limitations of a different kind, however, apply to the present two-dimensional scheme. The data on which the scheme is based were obtained with a restricted range of stimulus configurations. It is to be expected that the simple summation scheme will need elaboration if it is to account for more complex motion phenomena. For example, we have not considered stimulus configurations that produce

concurrent percepts of motion in more than one direction (e.g. Adelson & Movshon, 1982).

Similar limitations apply to our examination of bandwidth effects. Linear summation may well be limited to populations of sensors in neighbouring frequency bands. For nonadjacent frequency bands, or for compound stimuli differing along other salient dimensions such as contrast (e.g. Adelson & Movshon, 1982), summation may well exhibit the kind of nonlinearities recently described by Ferrera and Wilson (1990). It remains to be seen whether such nonlinearities can be incorporated in a more general version of the present scheme.

Acknowledgements—This work was supported by operating grants no. OGP38521 (to WFB) and no. A6592 (to VDL) from the Natural Sciences and Engineering Research Council of Canada. We thank Michael J. Morgan and Curtis L. Baker for helpful comments on an earlier version of this paper.

REFERENCES

Adelson, E. H. & Bergen, J. R. (1985). Spatiotemporal energy models for the perception of motion. *Journal of the Optical Society of America, 2A*, 284–299.

Adelson, E. H. & Movshon, J. A. (1982). Phenomenal coherence of moving visual patterns. *Nature, London, 300*, 523–525.

Baker, C. L. Jr, Baydala, A. & Zeitouni, N. (1989). Optimal displacement in apparent motion. *Vision Research, 29*, 849–859.

Bischof, W. F. & Di Lollo, V. (1990). Perception of directional sampled motion in relation to displacement and spatial frequency: Evidence for unitary motion system. *Vision Research, 30*, 1341–1362.

Braddick, O. (1974). A short-range process in apparent motion. *Vision Research, 14*, 519–527.

Burr, D. C., Ross, J. & Morrone, C. (1986). Smooth and sampled motion. *Vision Research, 26*, 643–652.

Chang, J. J. & Julesz, B. (1983). Displacement limit for spatial frequency filterd random-dot cinematograms in apparent motion. *Vision Research, 23*, 1379–1385.

Chang, J. J. & Julesz, B. (1985). Cooperative and non-cooperative processes of apparent movement of random-dot cinematograms. *Spatial Vision, 1*, 39–45.

Cleary, R. & Braddick, O. J. (1987). Apparent motion in one- and two-dimensional band-pass images. *Perception, 16*, A38.

Cleary, R. & Braddick, O. J. (1990a) Direction discrimination for band-pass filtered random dot kinematograms. *Vision Research, 30*, 303–316.

Cleary, R. & Braddick, O. J. (1990b). Masking of low frequency information in short-range apparent motion. *Vision Research, 30*, 317–327.

Dawson, M. & Di Lollo, V. (1990). Effects of adapting luminance and stimulus contrast on the temporal and spatial limits of short-range motion. *Vision Research, 30*, 415–429.

Ferrera, V. P. & Wilson, H. R. (1990). Perceived direction of moving two-dimensional patterns. *Vision Research, 30*, 273–287.

Finley, G. (1985). A high-speed point plotter for vision research. *Vision Research, 25*, 1993–1997.

Marr, D. & Ullman, S. (1981). Directional selectivity and its use in early visual processing. *Proceedings of the Royal Society, London, 211B*, 151–180.

Morgan, M. J. (1980). Spatiotemporal filtering and the interpolation effect in apparent motion. *Perception, 9*, 161–174.

Nakayama, K. & Silverman, G. H. (1985). Detection and discrimination of sinusoidal grating displacements. *Journal of the Optical Society of America, 2A*, 267–274.

Reichardt, W. (1961). Autocorrelation, a principle for the evaluation of sensory information. In Rosenblith, W. A. (Ed.), *Sensory communication*. Cambridge, MA: MIT Press.

Taylor, M. M. & Creelman, C. D. (1967). PEST: Efficiency estimates on probability functions. *Journal of the Acoustical Society of America, 41*, 782–787.

Turano, K. & Pantle, A. (1985). Discontinuity limits for the generation of visual motion aftereffects with sine- and square-wave gratings. *Journal of the Optical Society of America, 2A*, 260–266.

Van Santen, J. P. H. & Sperling, G. (1985). Elaborated Reichardt detectors. *Journal of the Optical Society of America, 2A*, 300–320.

Watson, A. B. & Ahumada, A. J. (1985). Model of human visual-motion sensing. *Journal of the Optical Society of America, 2A*, 322–341.

Watson, A. B., Ahumada, A. J. & Farrell, J. E. (1986). Window of visibility: A psychophysical theory of fidelity in time-sampled visual motion displays. *Journal of the Optical Society of America, 3*, 300–307.